Supplementary figures for "Underestimation of global O_2 loss in optimally interpolated historical ocean observations"

Takamitsu Ito[1], Hernan E. Garcia[2], Zhankun Wang[2], Shoshiro Minobe[3,4], Matthew C. Long[5], Just Cebrian[2,6], James Reagan[2], Tim Boyer[2], Christopher Paver[2], Courtney Bouchard[2], Yohei Takano[7], Seth Bushinsky[8], Ahron Cervania[1], Curtis A. Deutsch[9]

[1]School of Earth and Atmospheric Sciences, Georgia Institute of Technology, Atlanta, Georgia USA
[2]NOAA, National Centers for Environmental Information, Silver Springs, Maryland, USA
[3]Department of Natural History Sciences, Graduate School of Science, Hokkaido University, Sapporo, Japan
[4]Department of Earth and Planetary Sciences, Faculty of Science, Hokkaido University, Sapporo, Japan
[5]Climate and Global Dynamics, National Center for Atmospheric Research, Boulder, Colorado, USA
[6]Northern Gulf Institute, Mississippi State University, Stennis Space Center, Mississippi, USA
[7]Los Alamos National Laboratory, Los Alamos, New Mexico, USA
[8]School of Ocean and Earth Science and Technology, University of Hawaii at Manoa, Honolulu, Hawaii, USA
[9]Department of Geosciences, Princeton University, Princeton, NJ, USA

Correspondence to: Taka Ito (taka.ito@eas.gatech.edu)

Supplementary Figures

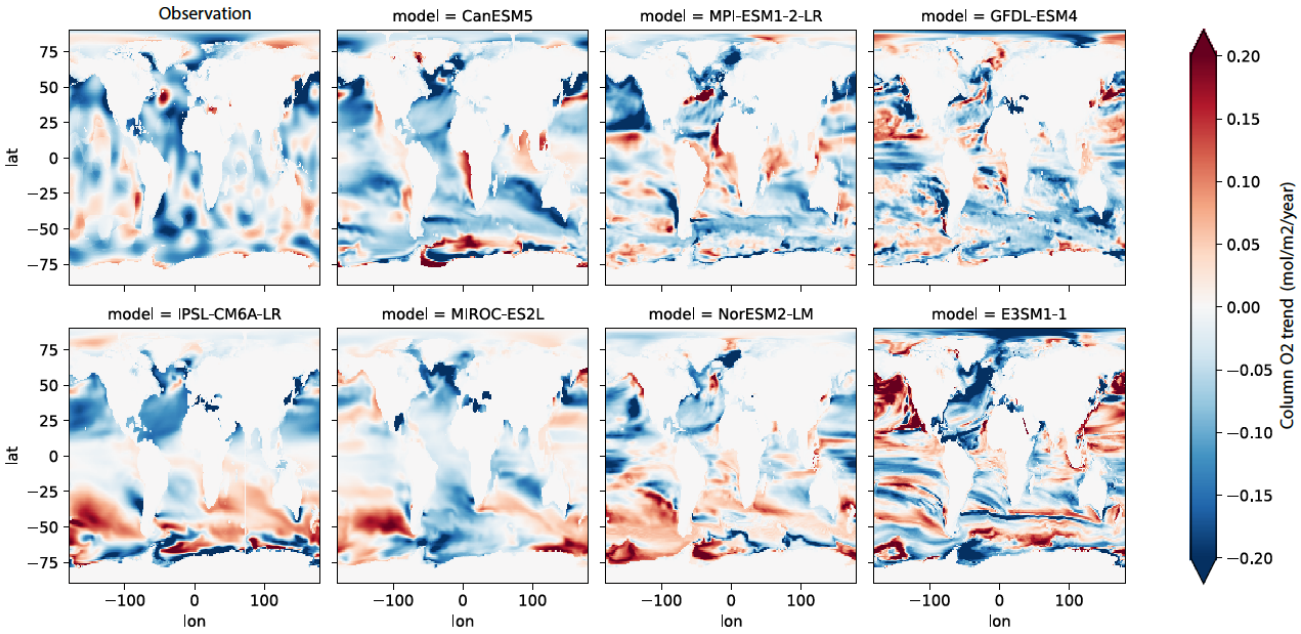

Supplementary Figure S1. Upper ocean (0-1,000m) column O_2 trend from 1967 to 2012. From upper left to lower right panel, observation (World Ocean Database 2018), CanESM5, MPI-ESM1-2-LR, GFDL-ESM4, IPSL-CM6A-LR, MIROC-ES2L, NorESM2-LM, and E3SM1-1. The full model output is used to calculate the model-derived O_2 trend.

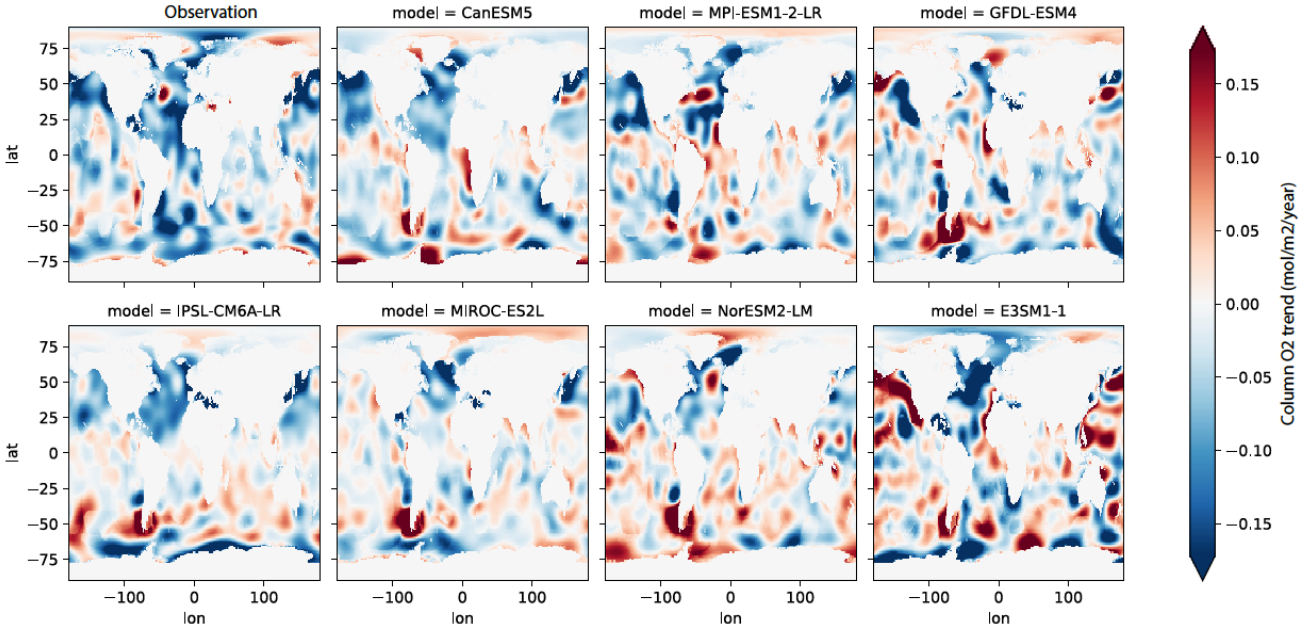

Figure S2. Upper ocean (0-1,000m) column O_2 trend from 1967 to 2012. From upper left to lower right panel, observation (World Ocean Database 2018), CanESM5, MPI-ESM1-2-LR, GFDL-ESM4, IPSL-CM6A-LR, MIROC-ES2L, NorESM2-LM, and E3SM1-1. The sub-sampled and optimally interpolated model output is used to calculate the model-derived O_2 trend.

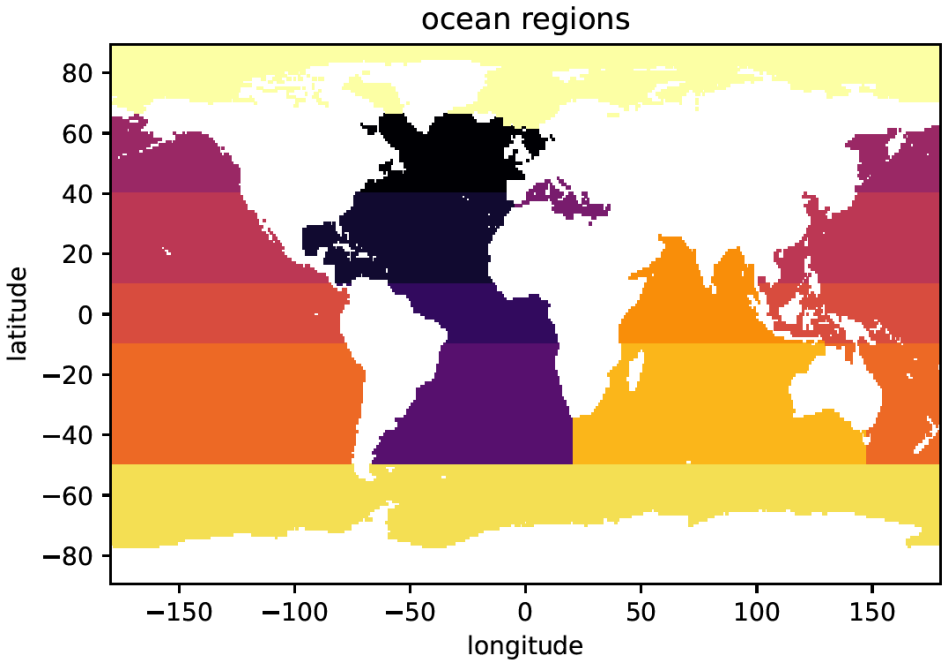

Figure S3. Ocean regions used in the inventory calculations. The global ocean is divided into 13 regions including [1] Subpolar North Atlantic (SPNA), [2] Subtropical North Atlantic (STNA), [3] Equatorial Atlantic (EQAT), [4] Subtropical South Atlantic (STSA), [5] Mediterranean Sea (MED), [6] Subpolar North Pacific (SPNP), [7] Subtropical North Pacific (STNP), [8] Equatorial Pacific (EQPA), [9] Subtropical South Pacific (STSP), [10] Equatorial Indian Ocean (EQID), [11] Subtropical South Indian Ocean (STSI), [12] Southern Ocean (SO), [13] Arctic Ocean (AO).

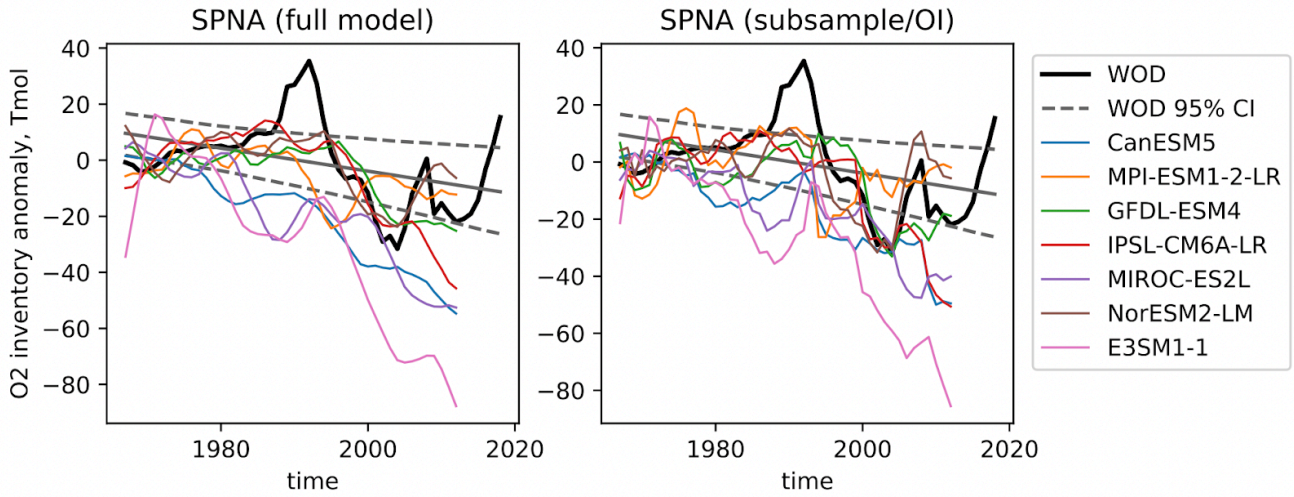

Figure S4. Time series of Subpolar North Atlantic (SPNA) upper ocean (0-1,000m) column O_2 inventory from World Ocean Database 2018 (black solid) and CMIP6 models (color) from (left) full model output and (right) subsampled and optimally interpolated model output.

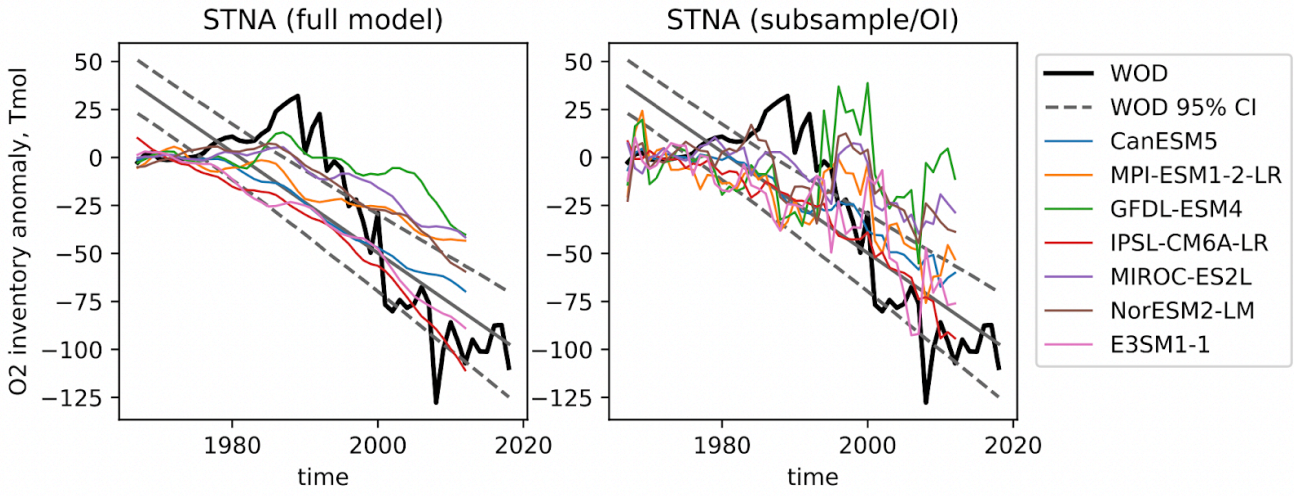

Figure S5. Time series of Subtropical North Atlantic (STNA) upper ocean (0-1,000m) column O_2 inventory from World Ocean Database 2018 (black solid) and CMIP6 models (color) from (left) full model output and (right) subsampled and optimally interpolated model output.

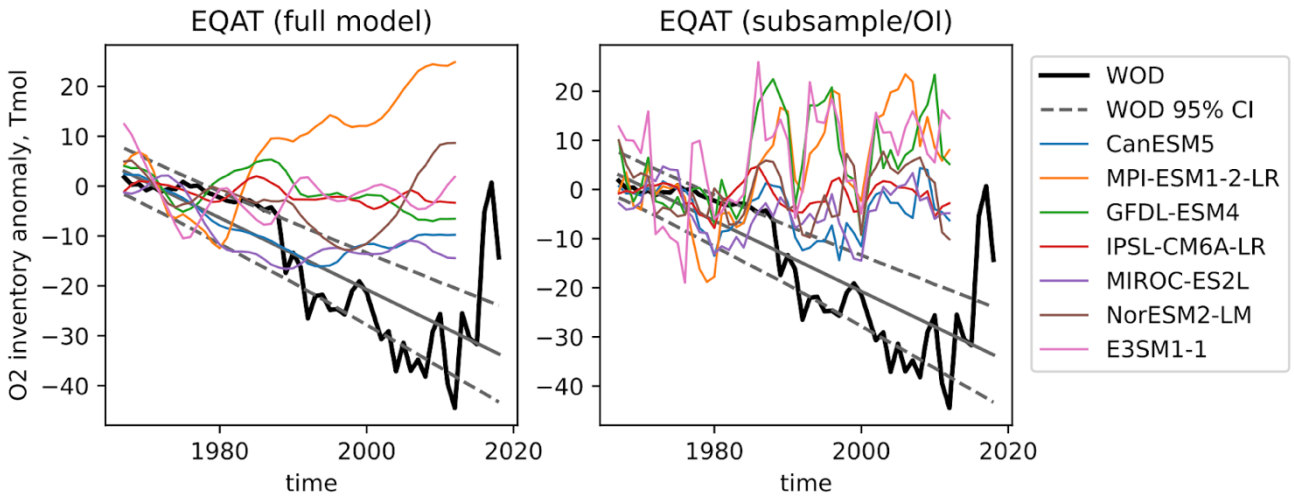

Figure S6. Time series of Equatorial Atlantic (EQAT) upper ocean (0-1,000m) column O_2 inventory from World Ocean Database 2018 (black solid) and CMIP6 models (color) from (left) full model output and (right) subsampled and optimally interpolated model output.

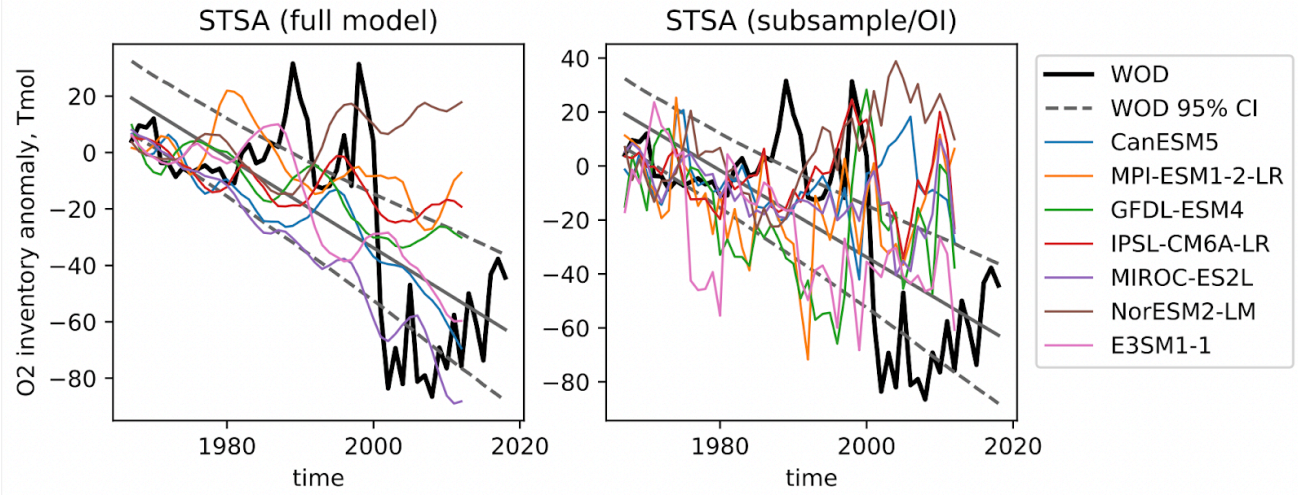

Figure S7. Time series of Subtropical South Atlantic (STSA) upper ocean (0-1,000m) column O_2 inventory from World Ocean Database 2018 (black solid) and CMIP6 models (color) from (left) full model output and (right) subsampled and optimally interpolated model output.

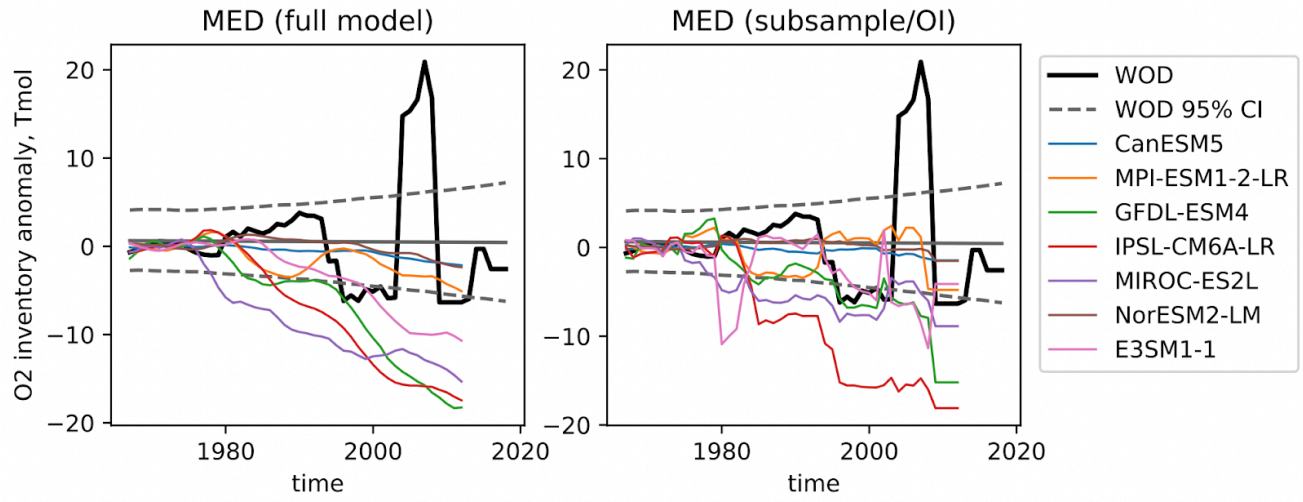

Figure S8. Time series of Mediterranean (MED) upper ocean (0-1,000m) column O_2 inventory from World Ocean Database 2018 (black solid) and CMIP6 models (color) from (left) full model output and (right) subsampled and optimally interpolated model output.

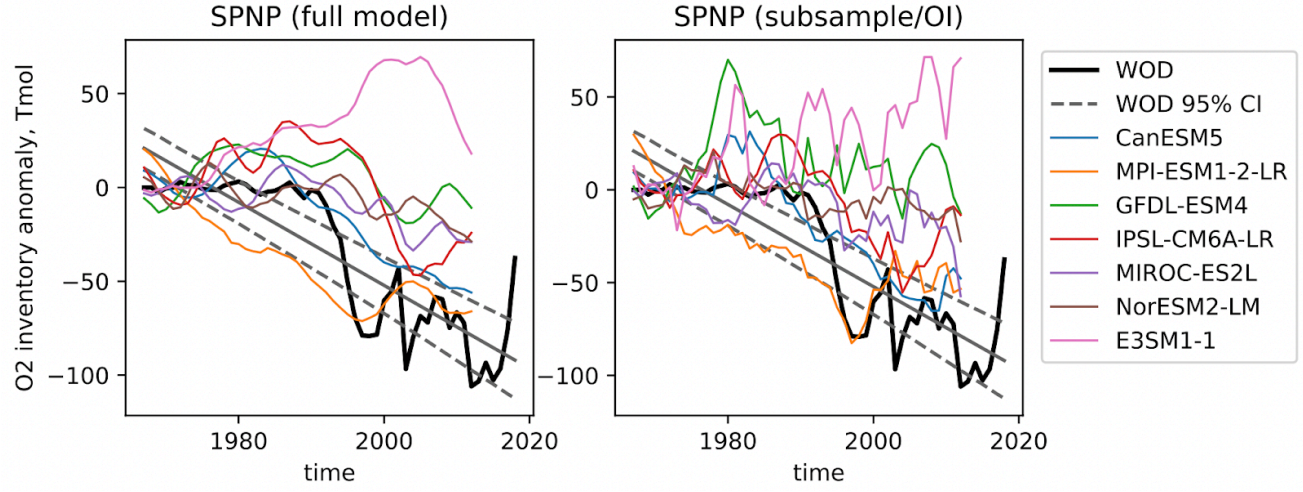

Figure S9. Time series of Subpolar North Pacific (SPNP) upper ocean (0-1,000m) column O_2 inventory from World Ocean Database 2018 (black solid) and CMIP6 models (color) from (left) full model output and (right) subsampled and optimally interpolated model output.

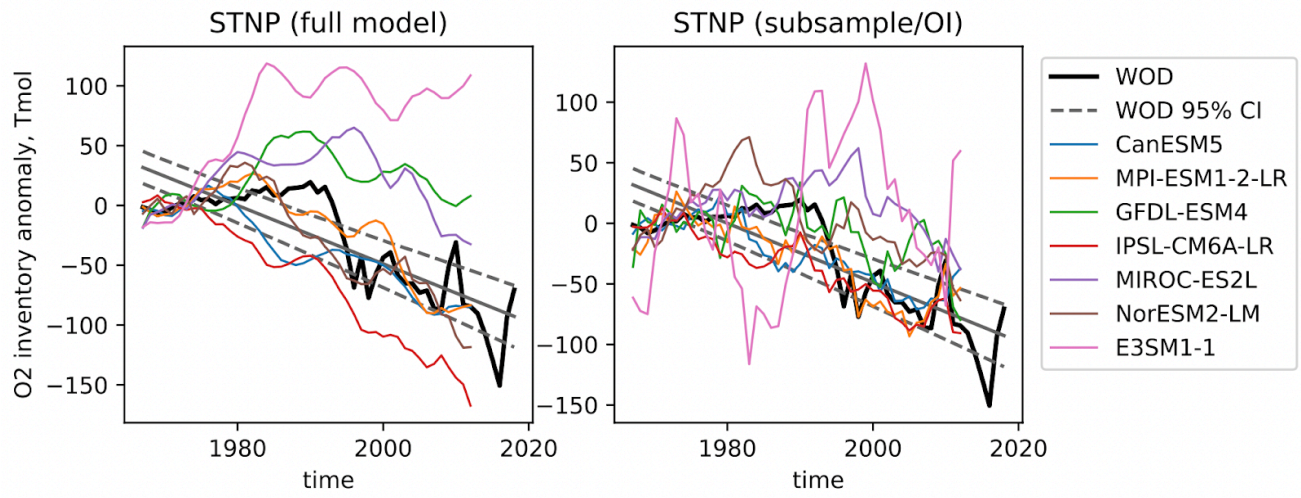

Figure S10. Time series of Subtropical North Pacific (STNP) upper ocean (0-1,000m) column O_2 inventory from World Ocean Database 2018 (black solid) and CMIP6 models (color) from (left) full model output and (right) subsampled and optimally interpolated model output.

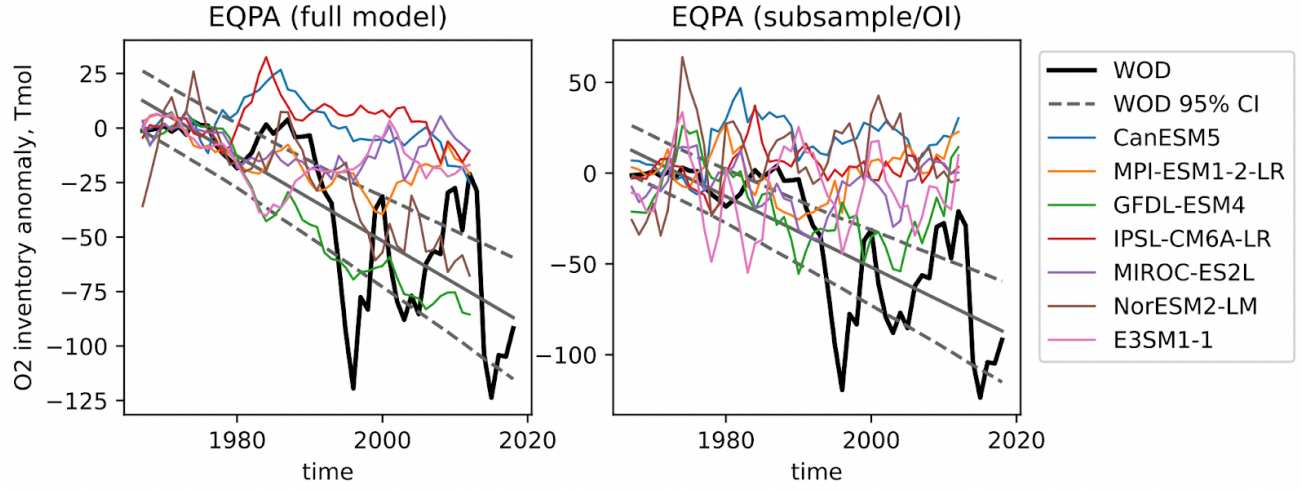

Figure S11. Time series of Equatorial Pacific (EQPA) upper ocean (0-1,000m) column O_2 inventory from World Ocean Database 2018 (black solid) and CMIP6 models (color) from (left) full model output and (right) subsampled and optimally interpolated model output.

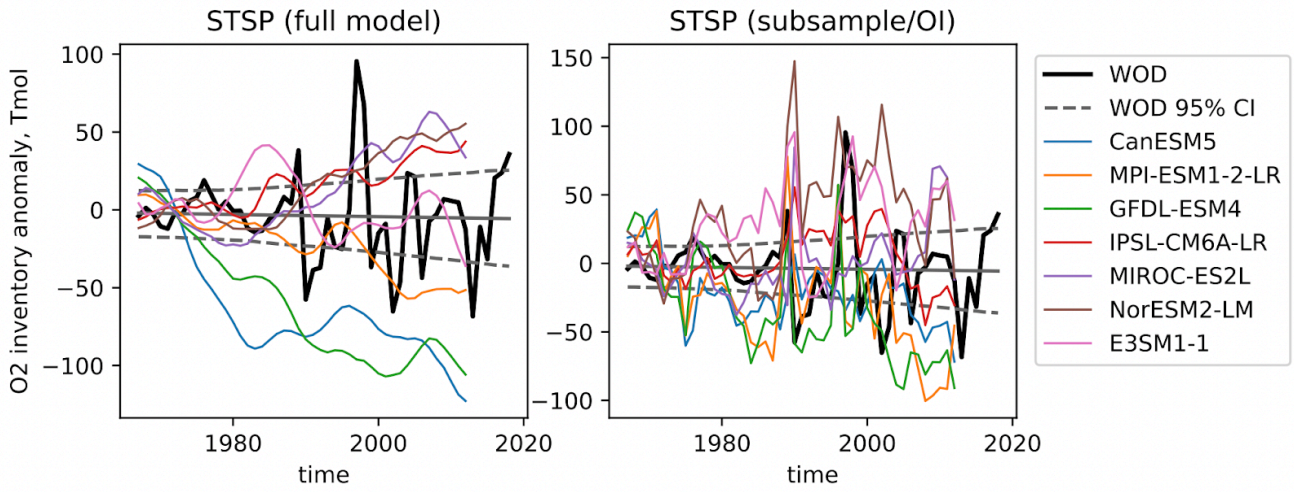

Figure S12. Time series of Subtropical South Pacific (STSP) upper ocean (0-1,000m) column O_2 inventory from World Ocean Database 2018 (black solid) and CMIP6 models (color) from (left) full model output and (right) subsampled and optimally interpolated model output.

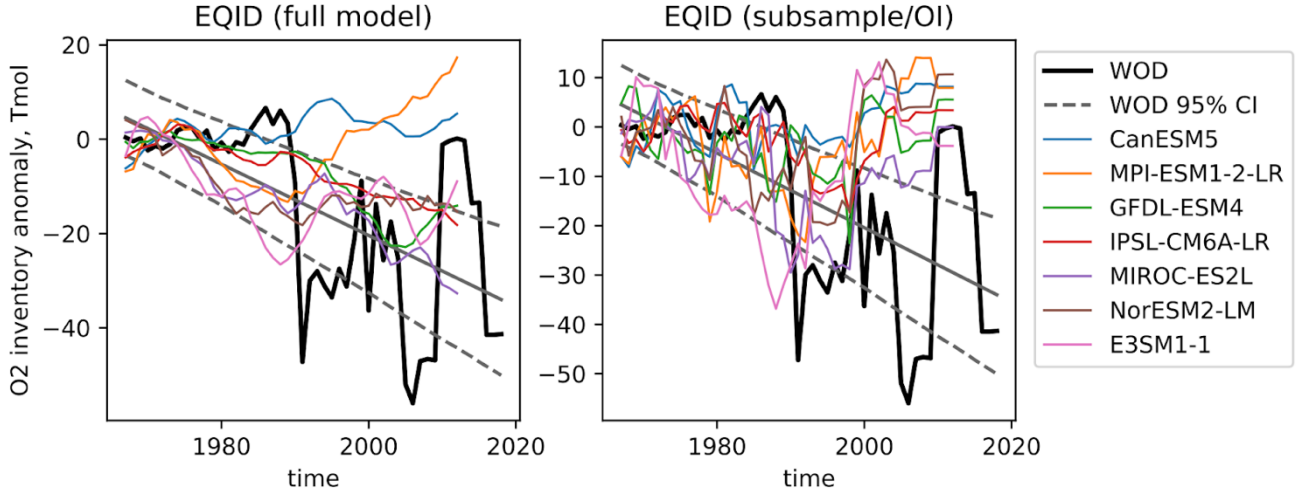

Figure S13. Time series of Equatorial Indian (EQID) upper ocean (0-1,000m) column O_2 inventory from World Ocean Database 2018 (black solid) and CMIP6 models (color) from (left) full model output and (right) subsampled and optimally interpolated model output.

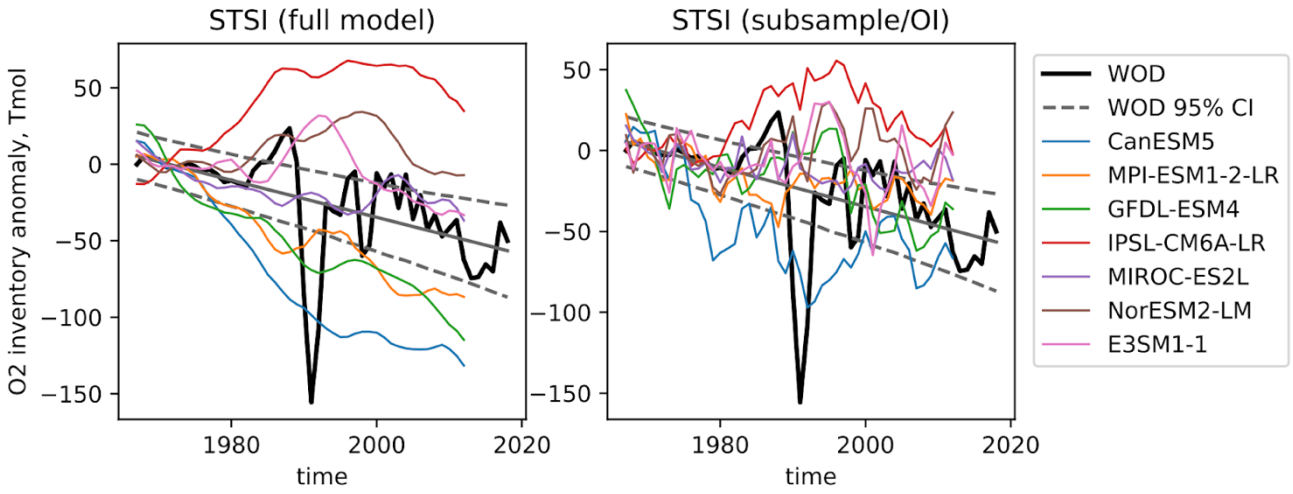

Figure S14. Time series of Subtropical South Indian (STSI) upper ocean (0-1,000m) column O_2 inventory from World Ocean Database 2018 (black solid) and CMIP6 models (color) from (left) full model output and (right) subsampled and optimally interpolated model output.

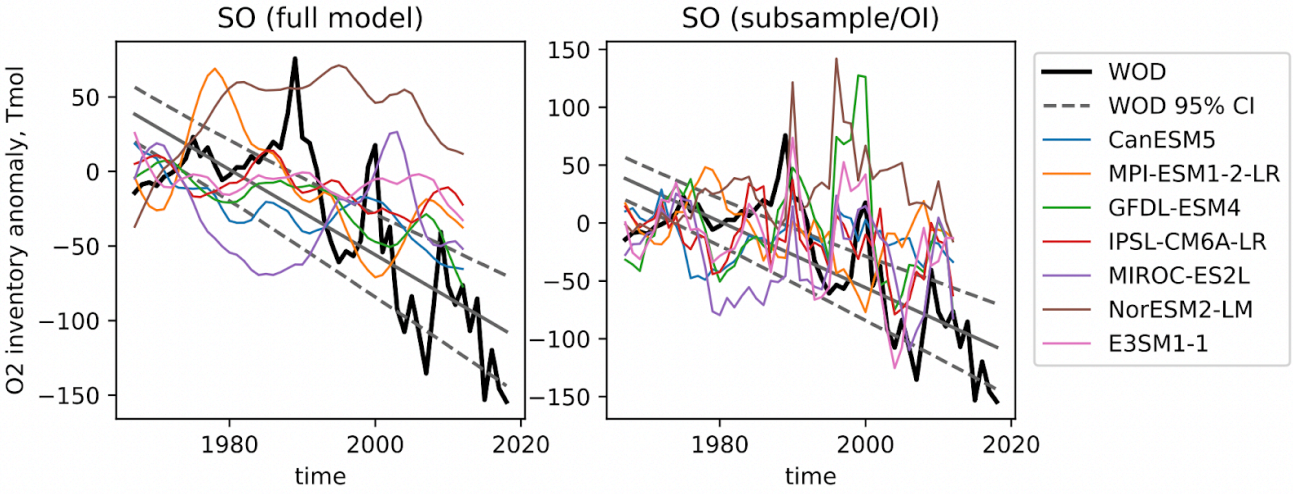

Figure S15. Time series of Southern Ocean (SO) upper ocean (0-1,000m) column O_2 inventory from World Ocean Database 2018 (black solid) and CMIP6 models (color) from (left) full model output and (right) subsampled and optimally interpolated model output.

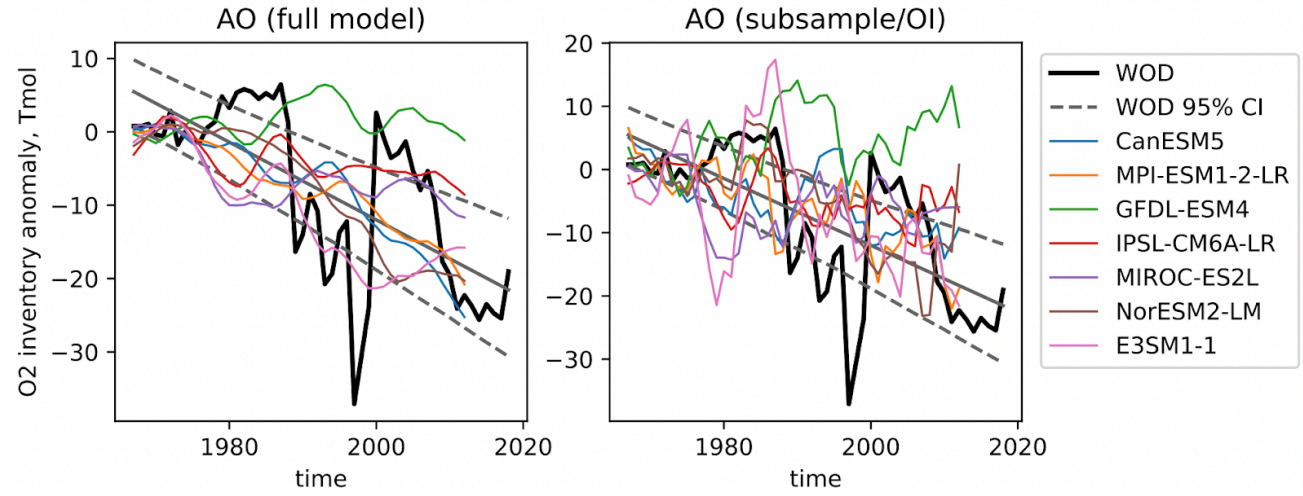

Figure S16. Time series of Arctic Ocean (AO) upper ocean (0-1,000m) column O_2 inventory from World Ocean Database 2018 (black solid) and CMIP6 models (color) from (left) full model output and (right) subsampled and optimally interpolated model output.

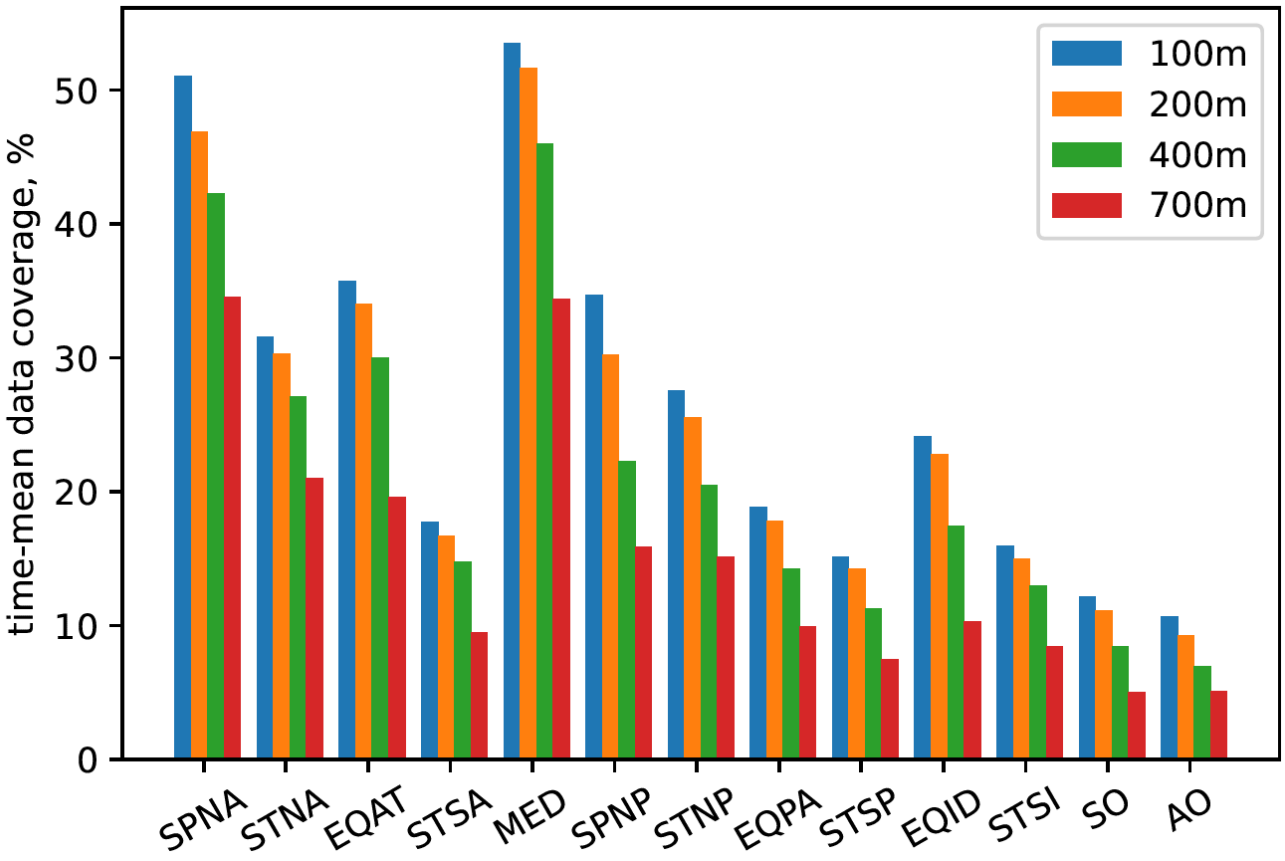

Figure S17. Time-mean data coverage for each basin at the depths of 100, 200, 400 and 700m.

130